THE JOURNAL OF BIOLOGICAL CHEMISTRY VOL. 287, NO. 13, pp. 10379–10393, March 23, 2012

NADPH Oxidase-derived Reactive Oxygen Species Increases Expression of Monocyte Chemotactic Factor Genes in Cultured Adipocytes*

Received for publication, September 16, 2011, and in revised form, January 24, 2012 Published, JBC Papers in Press, January 27, 2012, DOI 10.1074/jbc.M111.304998

Chang Yeop Han[‡§], Tomio Umemoto[‡§], Mohamed Omer[‡§], Laura J. Den Hartigh[‡§], Tsuyoshi Chiba[‡§], Renee LeBoeuf[‡§], Carolyn L. Buller[¶], Ian R. Sweet[‡§], Subramaniam Pennathur[¶], E. Dale Abel[‖1], and Alan Chait[‡§2]

From the [‡]Division of Metabolism, Endocrinology and Nutrition, Department of Medicine, and [§]Diabetes and Obesity Center of Excellence, University of Washington, Seattle, Washington 98195-6426, the [‖]Division of Endocrinology, Metabolism and Diabetes and the Program in Molecular Medicine, University of Utah School of Medicine, Salt Lake City, Utah 84112, and the [¶]Division of Nephrology, Department of Medicine, University of Michigan, Ann Arbor, Michigan 48105

Background: Excess nutrients induce adipose inflammation.
Results: Excess glucose and palmitate generate ROS via NOX4 by a mechanism that involves the PPP and translocation of NOX4 into LRs, rather than by mitochondrial oxidation.
Conclusion: NOX4 activates monocyte chemotactic factor expression.
Significance: Understanding the source of ROS generation may lead to the development of new therapeutic targets for adipose tissue inflammation.

Excess glucose and free fatty acids delivered to adipose tissue causes local inflammation, which contributes to insulin resistance. Glucose and palmitate generate reactive oxygen species (ROS) in adipocytes, leading to monocyte chemotactic factor gene expression. Docosahexaenoate (DHA) has the opposite effect. In this study, we evaluated the potential sources of ROS in the presence of excess nutrients. Differentiated 3T3-L1 adipocytes were exposed to palmitate and DHA (250 μM) in either 5 or 25 mM glucose to evaluate the relative roles of mitochondrial electron transport and NADPH oxidases (NOX) as sources of ROS. Excess glucose and palmitate did not increase mitochondrial oxidative phosphorylation. However, glucose exposure increased glycolysis. Of the NOX family members, only NOX4 was expressed in adipocytes. Moreover, its activity was increased by excess glucose and palmitate and decreased by DHA. Silencing NOX4 inhibited palmitate- and glucose-stimulated ROS generation and monocyte chemotactic factor gene expression. NADPH, a substrate for NOX, and pentose phosphate pathway activity increased with glucose but not palmitate and decreased with DHA exposure. Inhibition of the pentose phosphate pathway by glucose-6-phosphate dehydrogenase inhibitors and siRNA suppressed ROS generation and monocyte chemotactic factor gene expression induced by both glucose and palmitate. Finally, both high glucose and palmitate induced NOX4 translocation into lipid rafts, effects that were blocked by DHA. Excess glucose and palmitate generate ROS via NOX4 rather than by mitochondrial oxidation in cultured adipocytes. NOX4 is regulated by both NADPH generated in the PPP and translocation of NOX4 into lipid rafts, leading to expression of monocyte chemotactic factors.

Excess energy derived from glucose or fatty acids leads to obesity, which is characterized by accumulation of macrophages in adipose tissue in response to chemotactic factors generated by adipocytes (1–3). Both adipocytes and macrophages secrete a number of pro-inflammatory molecules, which may lead to insulin resistance and chronic low grade inflammation (4–6). Production of reactive oxygen species (ROS)[3] has recently been implicated as an important contributor to the pathogenesis of obesity-associated insulin resistance (7, 8). In diabetes, it has been suggested that excess free fatty acid (FFA) increases ROS production, which in turn interferes with insulin signaling (9, 10). ROS have been considered to be mediators of signal transduction pathways that activate NFκB (11). Recently, we showed that ROS were generated by adipocytes after exposure to excess glucose and certain saturated fatty acids (SFAs) such as palmitate, and we showed that the generation of ROS was linked to NFκB activation and expression of the monocyte chemotactic factor genes, serum amyloid A3 (SAA3) and monocyte chemotactic protein-1 (MCP-1) (12). Quenching ROS with antioxidants or exposure of cells to certain polyunsaturated fatty acids (PUFA) such as DHA inhibited those

* This work was supported, in whole or in part, by National Institutes of Health Grants HL-094352, P30-DK-035816, DK-082841, and DK-089503 (to S. P.), and DK-17047.
[1] Established investigator of the American Heart Association and supported by the American Diabetes Association and National Institutes of Health Grant DK092065.
[2] To whom correspondence should be addressed: Division of Metabolism, Endocrinology and Nutrition, Diabetes and Obesity Center of Excellence, 815 Mercer St., Box 358055, University of Washington, Seattle, WA 98195-6426. Tel.: 206-543-3158; Fax: 206-543-3567; E-mail: achait@u.washington.edu.

[3] The abbreviations used are: ROS, reactive oxygen species; G6PD, glucose-6-phosphate dehydrogenase; NFκB, nuclear factor-κB; NOX, NADPH oxidase; PUFA, polyunsaturated fatty acids; PPP, pentose phosphate pathway; FFA, free fatty acids; SFA, saturated fatty acids; IBX, 3-isobutyl-1-methylxanthine; DHA, docosahexaenoate; LR, lipid raft; SOD, superoxide dismutase; MβCD, methyl-β-cyclodextrin; DHEA, dehydroepiandrosterone; 6-AN, 6-aminonicotinamide; MRM, multiple reaction monitoring; DPI, diphenyleneiodonium; CM-H_2DCFDA, 5- (and -6) chloromethyl-2′,7′-dichlorofluorescein diacetate.

events (12). Thus, the glucose- and palmitate-stimulated ROS generation appears to play an important role in adipocyte inflammation. However, the mechanisms by which excess glucose and SFAs generate ROS and how some PUFA inhibit ROS generation remain to be determined. ROS can be generated by overloading the mitochondrial oxidative phosphorylation system with metabolites from glucose and FFA and also by NADPH oxidases (NOX). To understand how inflammation arises as a basis for the development of therapeutic strategies, we endeavored to identify the source of ROS generated by nutrient excess.

NOX are membrane-bound enzyme complexes that transfer electrons from the NADPH to oxygen, producing superoxide and H_2O_2 (13). Among the seven isoforms of NOX, only NOX4 has no need of other activators and has sustained activity (13). Recent evidence implicates NOX4 in tissue repair and fibrogenesis (14). Although the proteins in the NOX family have effects on vascular smooth muscle, endothelial, and neural cells (15–17), we strove to characterize the role of the NOX family of enzymes in adipocyte biology, because of the pathophysiological implications of a role of NOX-derived ROS in obesity.

In this study, we show that excess glucose and palmitate generates ROS via NOX4 rather than by mitochondrial oxidation in differentiated 3T3-L1 adipocytes. NOX4-derived ROS generation was regulated by a mechanism that involved the pentose phosphate pathway (PPP) and translocation of NOX4 into lipid rafts, leading to monocyte chemotactic factor expression, whereas DHA had an inhibitory effect.

EXPERIMENTAL PROCEDURES

Reagents and Cell Culture—Palmitate (16:0), docosahexaenoate (DHA; 22:6), 3-isobutyl-1-methylxanthine, lucigenin, cytochrome *c*, dehydroepiandrosterone (DHEA), 6-aminonicotinamide (6-AN), methyl-β-cyclodextrin (MβCD), catalase, and superoxide dismutase (SOD) were purchased from Sigma. Intracellular ATP content was measured using the CellTiter-Glo Luminescent Cell Viability Assay (Promega) according to the manufacturer's protocol. 3T3-L1 murine preadipocytes, obtained from American Type Tissue Culture Collection, were propagated and differentiated according to standard procedures (18) with the exception that medium contained either 5 or 25 mM glucose with or without 250 μM FFA that was replenished daily.

Preparation of Fatty Acid-Albumin Complexes—FFAs were prepared by conjugation with albumin, as described previously (12).

Multiplex Real Time Quantitative Reverse Transcription-PCR—Real time reverse transcription-PCR (RT-PCR) was performed using the TaqMan Master kit (Applied Biosystems) in the ABI prism 7900HT system (19, 20). *Saa3*, *Mcp-1*, *Ucp-1, -2*, and *-3*, *Nox1–5, Duox 1/2*, glucose-6-phosphate dehydrogenase (*G6pd*), and carnitine palmitoyltransferase-1α (*CPT1α*) primers and a fluorescein amidite (FAM) probe were obtained from Applied Biosystems (Assay-on-Demand). Primers and TaqMan probes specific for *Gapdh* are as follows: for *Gapdh*, forward primer 5′AGCCTCGTCCCGTAGACAAA3′ and reverse primer 5′ACCAGGCGCCCAATACG3′; probe, HEX-5′AAATCCGTTCACACCGACCTTCACCA3′-BHQ1. Each sample was analyzed in triplicate and normalized in multiplex reactions using Gapdh as control.

In Vitro NOX4 and G6PD Gene Silencing—For experiments in which we tested the role of NOX4 and G6PD in mediating ROS generation and the expression of SAA3 and MCP-1, 2 days after completion of the differentiation protocol 3T3-L1 adipocytes were transiently transfected with small interfering RNA (siRNA) duplexes for NOX4 and G6PD or scrambled sequences, which were synthesized and purified by Ambion using the DeliverX System (Panomics), as described previously (19, 21).

Quantification of ROS—ROS generation was assessed as CM-H_2DCFDA (Molecular Probes) fluorescence, which was monitored by fluorescence-activated cell sorting (FACS) (FACSCanto, BD Biosciences) as described previously (22).

Detection of Mitochondrial Superoxide—To evaluate superoxide generation from mitochondria induced by high glucose and/or palmitate, MitoSOX Red reagent (Invitrogen) was used for staining 3T3-L1 adipocytes. MitoSOX Red is a live cell permeant that is rapidly and selectively targeted to mitochondria. Once in the mitochondria, MitoSOX is oxidized by superoxide and exhibits red fluorescence with absorption/emission maxima ~510/580 nm (23). Thus, we used MitoSOX as a mitochondrial "superoxide indicator" to compare mitochondrial ROS generation induced by excess glucose and palmitate. Briefly, cultured 3T3-L1 adipocytes were incubated with 5 μM MitoSOX for 20 min at 37 °C. At the same time, MitoTracker® Green (excitation/emission ~488/510 nm) was added to confirm intact mitochondrial membrane potential. After washing twice in PBS, DMEM without phenol red was added, and stained cells were analyzed by FACS or photographed by fluorescent microscopy (Nikon Eclipse 80i).

Measurement of Intermediary Metabolites—Intermediary metabolites from 3T3-L1 adipocytes were quantified by liquid chromatography-electrospray ionization-tandem mass spectrometry (LC/ESI-MS/MS) in the multiple reaction monitoring (MRM) mode as described previously for acyl-CoAs, acylcarnitines, and glycolytic and citric acid cycle species (24–26). Briefly, 3T3-L1 adipocytes were grown in 5 or 25 mM glucose-containing media for 7 days. The media were removed, and the metabolites were extracted with solvent (2.5:1:1 ratio of acetonitrile/methanol/isopropyl alcohol) containing stable isotope-labeled internal standards. Cell debris and precipitated proteins were removed, and the supernatant was subjected to MS analysis after reverse phase LC for acyl-CoAs on a ZORBAX SB-18 column (3.5 μm; Agilent Technologies) and acylcarnitines using a Symmetry C18 column (3.5 μm; Waters) and hydrophilic interaction chromatography for glycolytic and citric acid cycle metabolites with a Luna NH_2 column (3 μm; Phenomenex). The solvent system for LC separation for analysis of acyl-CoAs was as follows: solvent A, water/acetonitrile (95:5) in 15 mM ammonium hydroxide; solvent B, water/acetonitrile (10:90) in 15 mM ammonium hydroxide; for acylcarnitines, solvent A, 10 mM ammonium acetate in water; solvent B, 10 mM ammonium acetate in methanol; and for glycolytic and citric acid cycle intermediates solvent A, 5 mM ammonium acetate in water, pH 9.9, and solvent B, acetonitrile. An Agilent 6410 triple

quadrupole MS system equipped with an Agilent 1200 LC System and an ESI source was utilized. Glycolytic, citric acid cycle, acyl-CoA, and acylcarnitine species were each detected by their characteristic LC retention time in the MRM mode following ESI and comparing relative areas with those of corresponding standards. A known amount of heptadecanoyl-CoA (C17:0) was added into the biological samples to quantify palmitoyl-CoA (C16:0), stearoyl-CoA (C18:0), oleoyl-CoA (C18:1), arachidonoyl-CoA (20:4), and docosahexaenoyl-CoA (C22:6) by comparing the relative peak areas of the reconstructed ion chromatograms. Concentrations of carnitine, acetylcarnitine (C2), propionylcarnitine (C3), butyrylcarnitine (C4), isovalerylcarnitine (C5), hexanoylcarnitine (C6), octanoylcarnitine (C8), myristoylcarnitine (C14), and palmitoylcarnitine (C16) were calculated by ratios of peak areas of known concentrations of stable isotopically labeled analogs. Glycolytic and citric acid cycle intermediates, including fructose 1,6-bisphosphate (FBP), pyruvate, citrate, isocitrate, α-ketoglutarate, succinate, fumarate, malate, oxaloacetate, and phosphoenolpyruvate, were also evaluated by peak areas relative to those of isotopically labeled standards. Isomers glucose 6-phosphate/fructose 6-phosphate elute together as a single peak. Furthermore, both isomers have an identical MRM transition. Therefore, these two compounds could not be distinguished separately. Similarly, 2- and 3-phosphoglycerate have the same retention time and MRM transitions. Henceforth, both of these pairs of compounds cannot be individually quantified as the contribution of each of the isomer to a peak is unknown. The relative abundance of the combined peak of each of these isomers was determined by ion intensity of their peak areas. Data extraction and peak area analyses were performed using MassHunter software. Data were normalized to protein concentrations from cells measured by a bicinchoninic acid (BCA) protein assay (Thermo Scientific).

Measurement of Oxygen Consumption Rate and Lactate Production Rate—Assessment of oxygen consumption and lactate production by adipocytes was done using a previously developed islet flow culture system (27) where modifications were made to accommodate attached adipocytes. 3T3-L1 adipocytes (10^6 cells) were seeded on glass coverslips within a rectangle area (15 by 20 mm) on the upstream side of an area where a polymerized platinum porphyrin dye was affixed (28). The cells were then grown in culture media containing either 5 or 25 mM glucose for 7 days. Subsequently, the coverslip was placed into a temperature-controlled 100-ml perfusion dish (Bioptechs) that was mounted onto the stage of a Nikon Eclipse TE-200 inverted microscope, and Krebs-Ringer buffer was pumped through the dish at a flow rate of 50 μl/min. At 0 time, the solution containing 1 μM insulin, at which concentration uptake and phosphorylation of insulin receptor is maximized, was perfused through the chamber to monitor the insulin response (29). Fluorescent emission of the dye was detected at 610 nm by a Photometrics Cool Snap EZ camera (Photometrics) during excitation at 546 nm with a xenon lamp. Fluorescent signals were converted to oxygen concentrations by use of a calibration curve determined at the end of each experiment using tanks of gas with varying oxygen levels. Outflow fractions were collected and subsequently assayed for lactate using a kit purchased from Invitrogen (Amplex Red glucose/glucose oxidase assay kit) per the manufacturer's instructions except that lactate oxidase was substituted for glucose oxidase. Oxygen consumption and lactate production rates were calculated as the product of the flow rate and the difference between inflow and outflow levels of oxygen or lactate, respectively, divided by the number of cells. Inflow oxygen tension was determined at the end of each experiment by inhibiting cellular respiration with antimycin A.

Measurement of NOX Activity by SOD-inhibitable Chemiluminescence and Cytochrome c Reduction—3T3-L1 adipocytes were incubated for 10 min with hypotonic lysis buffer (25 mM Tris-HCl, 1 mM EDTA, 1 mM EGTA, protease inhibitor, pH 7.4), homogenized with 10 strokes of a loose fitting Dounce homogenizer, and centrifuged (1,000 × *g*, 4 °C, 15 min). The supernatant was ultracentrifuged at 100,000 × *g* for 60 min at 4 °C. The pellet, which contained the membrane fraction, was dissolved in suspension buffer (50 mM triethanolamine, 150 mM NaCl, 2 mM $MgCl_2$, 0.1 mM EGTA, protease inhibitor). Equal amounts of membrane fraction protein were incubated in PBS buffer with 100 units/ml catalase. For the chemiluminescence assay, lucigenin (5 μM) and NADPH (100 μM) were added and incubated for 10 min at 37 °C with or without SOD (125 units/ml) and recorded using a luminometer (Berthold). For cytochrome *c* reduction, cytochrome *c* (5 μM) and NADPH (100 μM) were added and incubated for 60 min at 37 °C with/without SOD (125 units/ml). Cytochrome *c* reduction was calculated using absorbance at 550 nm corrected for background reading at 540 and 560 nm.

Detergent-free Subcellular Fractionation—Lipid raft (LR) and non-LR fractions from adipocytes were obtained by Optiprep gradient centrifugation using a detergent-free protocol (30). Briefly, the cell pellet was homogenized in buffer (250 mM sucrose, 1 mM EDTA, 500 mM sodium bicarbonate, pH 11), with 15 strokes of a loose fitting Dounce homogenizer and sonicated (20 times for 30 s). After centrifugation (1,000 × *g*, 10 min), the post-nuclear supernatant fraction was added to 60% Optiprep to make 35% Optiprep (final concentration). The 35% Optiprep samples were overlaid with 5–35% OptiPrep as a discontinuous gradient and centrifuged at 60,000 rpm in a Beckman NVT 65.2 rotor for 90 min at 4 °C. After centrifugation, nine 0.5-ml fractions were collected using a fraction collector. The fractionated proteins were subjected to immunoblotting using antibodies against NOX4 (ABCAM) and caveolin-1 (Cell Signaling).

Measurement of Glucose Oxidation or β-Oxidation of Fatty Acids—To measure the PPP activity and β-oxidation, we used [1-^{14}C]glucose, [6-^{14}C]glucose, [1-^{14}C]oleate, or [1-^{14}C]palmitate (American Radiolabeled Chemicals Inc.) as described previously (31–33). Adipocytes were gently detached with nonenzymatic dissociation solution (Sigma), and cell viability was checked as described previously (12), counted using a hemocytometer, and suspended in Krebs-Ringer buffer containing 1 nM insulin and placed in vials. Wells containing cylinders of Whatman filter paper were suspended above the adipocyte-containing solution in vials. The vials were stoppered with rubber caps, gassed with 95% O_2, 5% CO_2, and 0.5 μCi of [1-^{14}C]glucose and [6-^{14}C]glucose for glucose oxidation, or [1-^{14}C]oleate or [1-^{14}C]palmitate for β-oxidation was injected into the vials. After incubation for 60 min at 37 °C, 200 μl of hyamine hydroxide was injected into the wells containing the filter paper, 200 μl

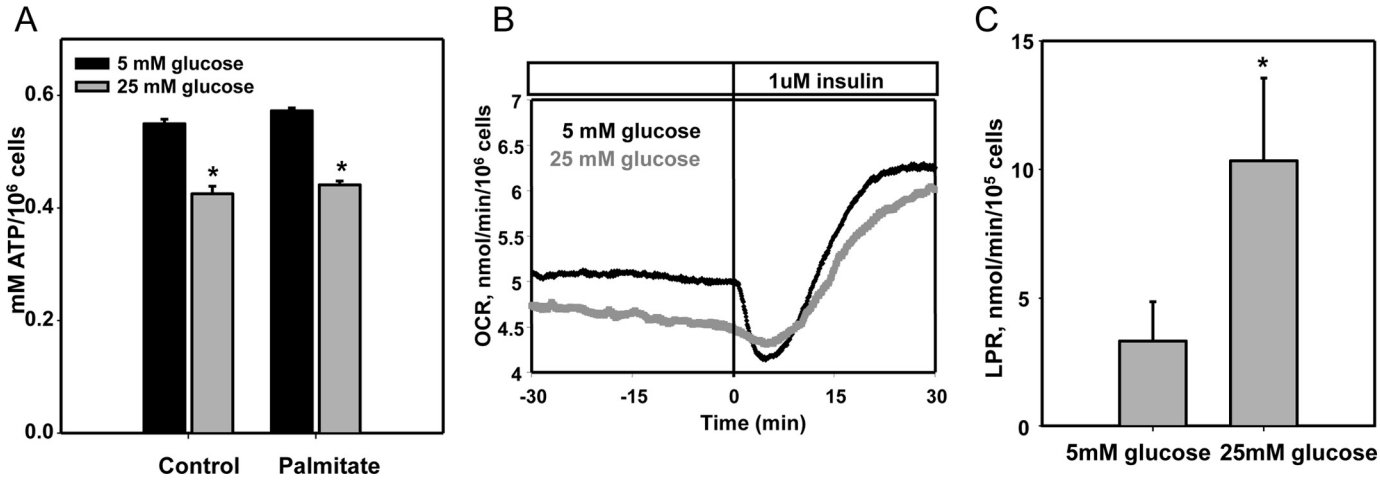

FIGURE 1. **Excess glucose and palmitate do not increase mitochondrial oxidative phosphorylation.** Differentiated 3T3-L1 adipocytes were cultured for 7 days in low (5 mM) or high (25 mM) glucose media with or without added palmitate (250 μM) as indicated. *A,* ATP content was measured by an ATP assay kit. Oxygen consumption rate (*B*) and lactate production rate (*LPR*) (*C*) were measured using a flow culture system as described under "Experimental Procedures." Oxygen consumption rate was measured in real time, and outflow samples were collected for lactate production rate and assayed for lactate, and the results were averaged over the duration of the experiment for the two separate conditions. *, $p < 0.001$ *versus* 5 mM glucose control.

of 1 N HCl was added to the adipocytes, and the vials were incubated overnight at 37 °C. The filter paper in the wells was then transferred to 10 ml of scintillation fluid and counted. Using this method, metabolized CO_2 from [1-^{14}C]glucose and [6-^{14}C]glucose, [1-^{14}C]oleate, and [1-^{14}C]palmitate was successfully trapped in hyamine-soaked filter papers. In the PPP, G6PD and 6-phosphogluconate dehydrogenase make NADPH and CO_2, which is derived from the first carbon of glucose. During glucose metabolism the first carbon only releases CO_2 from the PPP and the Krebs cycle. The Krebs cycle uses all carbons equivalently; therefore, CO_2 released from the 6-carbon of glucose will be the same as CO_2 from the 1-carbon of glucose. Thus, PPP activity can be measured by subtracting CO_2 labeled with 6-^{14}C (which is derived from the Krebs cycle) from CO_2 labeled with 1-^{14}C (derived from both the Krebs cycle and the PPP).

Animals, Diet, and Tissue Collection—Mice (*ob/ob, db/db,* and C57BL/6 littermate controls) were fed a chow diet for 24 weeks. At sacrifice, adipose tissues were snap-frozen at −70 °C, and total RNA was isolated for measurement of NOX4 gene expression. All experimental procedures were undertaken with approval from the Institutional Animal Care and Use Committees of the University of Washington and Tokyo Medical and Dental University.

Statistical Analysis—Statistical significance was determined by Student's *t* tests. All data are shown as means ± S.D. of three independent experiments performed in triplicate. $p < 0.05$ was considered significant.

RESULTS

Effect of Excess Glucose and Palmitate on Mitochondrial Oxidative Phosphorylation—We previously showed that daily replenishment of medium with 25 mM glucose or/and palmitate (250 μM) for 7 days resulted in increased ROS generation by differentiated 3T3-L1 adipocytes and was associated with NFκB activation and chemotactic factor expression (12). To test the hypothesis that excess glucose might overload the mitochondrial oxidation system, leading to leakage of electrons as a source of ROS, we first characterized the effect of chronic exposure to excess substrate on mitochondrial oxidative phosphorylation in 3T3-L1 adipocytes. Neither excess glucose nor palmitate increased intracellular ATP content (Fig. 1*A*), and oxygen consumption rate was not changed by chronic exposure to high glucose (Fig. 1*B*) suggesting that mitochondrial oxidation was not elevated during hyperglycemia. In fact, ATP content was actually slightly but significantly reduced by incubation with high glucose and palmitate. Because decreased ATP content could be due to an increase in uncoupling protein activity in mitochondria, we measured the gene expression of *Ucp-1, -2,* and *-3*. Ucp-2 was the major isoform detected in these cells and was not changed by excess glucose and palmitate. The expression of *Ucp-1* was undetectable, and the low expression level of *Ucp-3* was decreased by high glucose and palmitate (data not shown). In contrast to mitochondrial oxidative phosphorylation, which did not appear to increase in the presence of excess glucose, lactate production rate increased in response to high glucose (Fig. 1*C*), suggesting increased glycolysis occurs during chronic exposure to high glucose levels. β-Oxidation of FFAs could also be a potential source of mitochondrially derived ROS. We measured the expression level of *CPT1*α, the rate-limiting enzyme for fatty acid β-oxidation, and CO_2 release from [1-^{14}C]oleate and [1-^{14}C]palmitate as indices of fatty acid oxidation. Expression levels of CPT1α were suppressed by excess glucose and palmitate and restored by DHA (Fig. 2*A*). However, CO_2 production from [1-^{14}C]oleate or [1-^{14}C]palmitate through β-oxidation was not changed by exposure to high glucose or palmitate, although β-oxidation was increased by DHA (Fig. 2, *B* and *C*). These data suggest that β-oxidation is not involved in ROS generated by exposure of adipocytes to high glucose and palmitate. In support of these results, the Krebs cycle intermediary metabolites, acyl-CoA or acylcarnitines, did not change between low and high glucose conditions (Tables 1–3). However, 2,3-phosphoglycerate, an intermediary metabolite in glycolysis, increased after exposure of cells to high glucose (Fig. 2*D*).

TABLE 1

Intermediary metabolites from Krebs cycle

The targeted metabolomic analysis by LC/ESI/MS/MS was performed in extracts from 3T3-L1 adipocytes cultured in 5 or 25 mM glucose for 7 days as described under "Experimental Procedures." No significant difference in Krebs cycle was noted. $n = 5$.

	5 mM glucose	25 mM glucose
	nmol/mg protein	*nmol/mg protein*
Pyruvate	33.12 ± 28.34	33.52 ± 14.69
Fumarate	33.80 ± 14.60	33.10 ± 12.87
Malate	88.50 ± 15.79	76.06 ± 13.02
Citrate	4.84 ± 1.17	3.58 ± 0.69
Succinate	29.06 ± 3.00	27.40 ± 3.96
Phosphoenolpyruvate	28.29 ± 9.29	47.54 ± 14.51
Oxaloacetate	0.11 ± 0.01	0.10 ± 0.01
Isocitrate	0.14 ± 0.02	0.10 ± 0.02
α-Ketoglutarate	100.82 ± 14.09	74.30 ± 28.40

TABLE 2

Acyl-CoAs

The targeted metabolomic analysis by LC/ESI/MS/MS was performed in extracts from 3T3-L1 adipocytes cultured in 5 or 25 mM glucose for 7 days as described under "Experimental Procedures." No significant difference in β-oxidation intermediary metabolites, including acyl-CoA, was seen. $n = 5$.

	5 mM glucose	25 mM glucose
	pmol/mg protein	*pmol/mg protein*
Palmitoyl-CoA	44.23 ± 6.69	61.31 ± 11.98
Stearoyl-CoA	15.24 ± 1.62	17.13 ± 5.72
Oleoyl-CoA	146.88 ± 27.50	170.55 ± 22.32
Linoleoyl-CoA	28.07 ± 4.93	26.68 ± 4.88
Arachidonoyl-CoA	420.94 ± 74.45	346.18 ± 52.95
Docosahexaenoyl-CoA	9.92 ± 2.78	8.40 ± 1.56

TABLE 3

Acyl-carnitines and β-oxidation intermediary metabolites

The targeted metabolomic analysis by LC/ESI/MS/MS was performed in extracts from 3T3-L1 adipocytes cultured in 5 or 25 mM glucose for 7 days as described under "Experimental Procedures." No significant difference in β-oxidation intermediary metabolites, including acyl-carnitines, was seen. $n = 5$.

	5 mM glucose	25 mM glucose
	nmol/mg protein	*nmol/mg protein*
L-Carnitine	2.1679 ± 0.2395	2.3395 ± 0.3476
Acetyl-L-carnitine	0.3984 ± 0.0529	0.4496 ± 0.0706
Propionyl-L-carnitine	0.3258 ± 0.0504	0.3460 ± 0.0469
Butyryl-L-carnitine	0.0234 ± 0.0065	0.0308 ± 0.0054
O-Isovaleryl-L-carnitine	0.0115 ± 0.0019	0.0143 ± 0.0022
Octanoyl-L-carnitine	0.0005 ± 0.001	0.0006 ± 0.0001
Lauroyl-L-carnitine	0.0315 ± 0.0052	0.0459 ± 0.0033
Palmitoyl-L-carnitine	2.3952 ± 0.3612	3.1198 ± 0.7308

As an additional test of the contribution of increased mitochondrial substrate flux to the generation of superoxide, we also used the mitochondrion-specific superoxide indicator, MitoSOX Red to measure mitochondrial superoxide. Excess glucose and palmitate exposure did not increase MitoSOX-detectable superoxide. Mitochondrial integrity was confirmed using MitoTracker® Green, detected both by fluorescent microscopy and FACS analysis (Fig. 3, *A* and *B*). Conversely, 3-isobutyl-1-methylxanthine, a phosphodiesterase inhibitor that increases intracellular cAMP (34) and significantly stimulates mitochondrial oxidative metabolism, used as a positive control, led to a 10-fold increase of mitochondrial oxygen consumption (data not shown) as well as MitoSOX positive staining in mitochondria (Fig. 3*B*). Taken together, these results do not support a significant role for mitochondria in the production of ROS during exposure to excess glucose and palmitate.

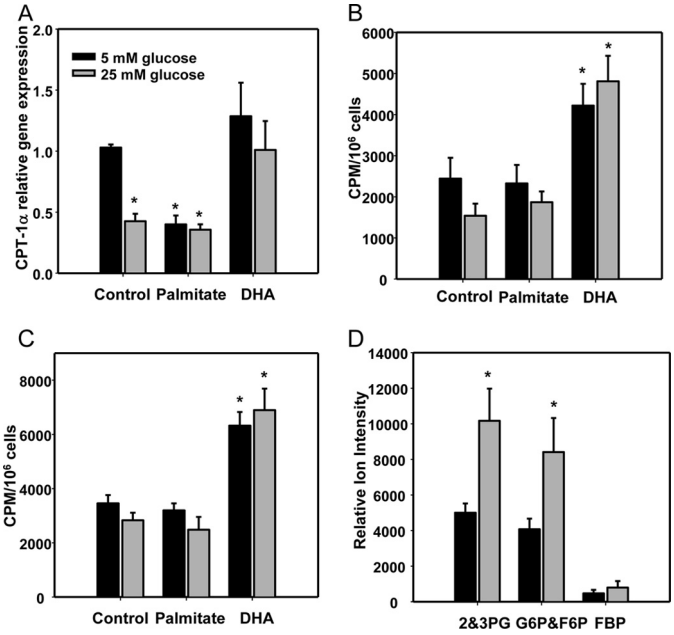

FIGURE 2. **β-Oxidation is not increased by excess glucose, palmitate, and DHA, although glycolytic pathway intermediates are increased by high glucose in 3T3-L1 adipocytes.** 3T3-L1 adipocytes were exposed to low or high glucose with or without palmitate or DHA (250 μM) for 7 days. *A,* total RNA was isolated and analyzed by multiplex real time RT-PCR using *Cpt-1α*-specific primers and normalized to *Gapdh*. Some cells were detached and put in vials for β-oxidation measurement with 0.5 μCi of [1-^{14}C]oleate or palmitate for 3 h. β-Oxidation was estimated as $^{14}CO_2$ production from [1-^{14}C]oleate (*B*) or [1-^{14}C]palmitate (*C*). *D,* targeted metabolomic analysis by LC/ESI-MS/MS was performed in extracts from 3T3-L1 adipocytes cultured in 5 or 25 mM glucose for 7 days as described under "Experimental Procedures." Incubation of cells in elevated glucose led to a 2-fold increase in glycolytic pathway intermediates, isomer pairs glucose 6-phosphate (G6P)/fructose 6-phosphate (F6P) and 2- and 3-phosphoglycerate (2&3PG). Relative abundance of these isomer pairs are expressed normalizing ion intensity of peak areas to protein content. *, $p < 0.001$ *versus* 5 mM glucose control.

NOX4 Is the Only Member of the NOX Family Expressed in Adipocytes and Its Activity Is Increased by High Glucose and Palmitate—The *Nox* family is another potential source of ROS generation. We measured mRNA expression levels of each NOX family member (*Nox1–5* and *Duox1/2*). Only NOX4 was expressed in differentiated 3T3-L1 adipocytes. Other NOX family members were detected at very low levels (Fig. 4*A*). Moreover, the mRNA expression and protein level of NOX4 were not changed by exposure to high glucose, palmitate, and/or DHA (Fig. 4, *B* and *C*).

To measure NOX activity in 3T3-L1 adipocytes, we isolated whole cell membrane fractions by ultracentrifugation. NOX activity was increased after exposure of cells to high glucose and palmitate and diminished by adding SOD (Fig. 5). Interestingly, DHA suppressed NOX activity induced by excess glucose and palmitate (Fig. 5). Because NOX4 is the only member of the NOX family expressed to any extent in adipocytes, we assumed this activity to be from NOX4.

Both Excess Glucose and Palmitate Stimulate NOX4-derived ROS—To investigate the role of NOX4 on ROS generation induced by high glucose and palmitate, NOX4 was silenced with a NOX4-specific siRNA. Following transfection of differentiated 3T3-L1 cells with a NOX4-specific siRNA, NOX4 expression levels were markedly silenced compared with transfection of control scrambled constructs and of untreated cells

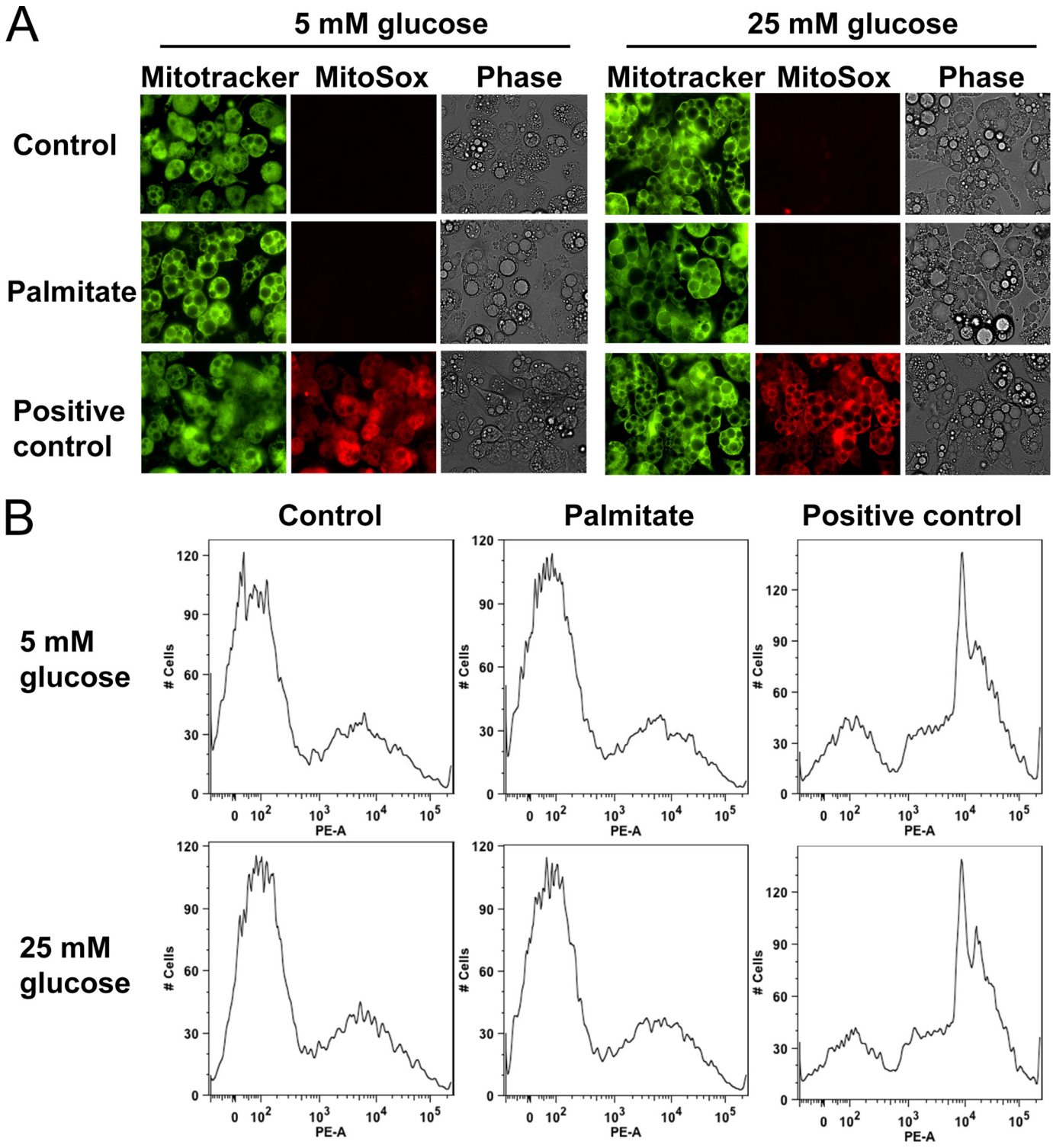

FIGURE 3. **ROS induced by excess glucose and palmitate is not generated from mitochondria in 3T3-L1 adipocytes.** Differentiated 3T3-L1 adipocytes were cultured for 7 days in low (5 mM) or high (25 mM) glucose media with or without added palmitate (250 μM) as indicated. Mitochondria were stained by MitoTracker Green and MitoSOX Red and photographed by fluorescent microscopy (Nikon Eclipse 80i, original magnification ×400) (*A*) or analyzed by FACS (*B*). The phosphodiesterase inhibitor, isobutyl-1-methylxanthine (5 μM), was used as a positive control for mitochondrial oxidative capacity (*A* and *B*).

(Fig. 6*A*). Because other NOX family members could undergo compensatory increases in NOX4-silenced adipocytes, we determined the expression of other *Nox* isoforms, none of which increased following NOX4 silencing (data not shown). Treatment with high glucose or palmitate could potentially increase other *Nox* isoforms and compensate for NOX4 silencing. However, none of the other isoforms were changed by exposure to glucose excess or palmitate (data not shown). We also measured ROS generation by FACS using CM-H_2DCFDA (Molecular Probes), a membrane-permeable dye that can be oxidized by intracellular ROS to the fluorescent product 5- (and -6) chloromethyl-2′,7′-dichlorofluorescein (CM-DCF) (35).

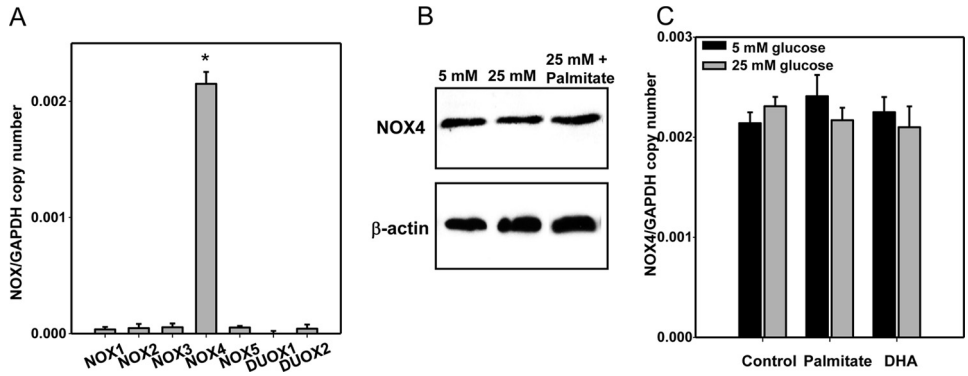

FIGURE 4. **NOX4 is the major isoform in 3T3-L1 adipocytes.** Differentiated 3T3-L1 adipocytes were cultured for 7 days in low or high glucose media with or without 250 μM of palmitate or DHA. Total RNA was isolated and analyzed by multiplex real time RT-PCR using various *Nox*-specific primers and probes as indicated (*A* and *C*) and normalized to *Gapdh*. NOX4 protein levels of cells were measured by immunoblot using an anti-NOX4 antibody (*B*). *, $p < 0.001$ *versus* *Nox1–3* and *-5* and *Duox1/2*.

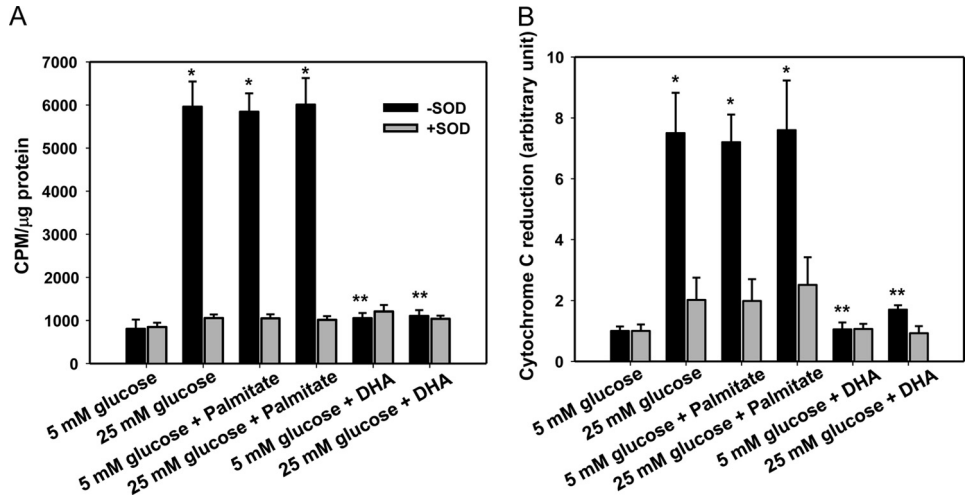

FIGURE 5. **NOX activity is increased by exposure of cells to excess glucose and palmitate, although activity is decreased by exposure of cells to DHA.** NADPH-dependent and SOD-inhibitable superoxide release was measured by lucigenin chemiluminescence (*A*) and reduction of cytochrome *c* (*B*) in differentiated 3T3-L1 adipocytes that were cultured for 7 days in low or high glucose media with or without 250 μM palmitate or DHA. *, $p < 0.001$ *versus* 5 mM glucose control; **, $p < 0.001$ *versus* 25 mM glucose control.

Daily exposure of cells to high glucose and palmitate for 7 days increased intracellular ROS generation (Fig. 6*B*). Silencing of NOX4 inhibited palmitate-derived as well as high glucose-derived ROS generation. In addition, ROS generation by palmitate in the presence of high glucose was partially inhibited by NOX4 silencing (Fig. 6*B*). To examine the role of NOX4 on the expression of chemotactic factor genes, we measured *Saa3* and *Mcp-1* gene expression after silencing NOX4. *Saa3* and *Mcp-1* gene expression induced by high glucose and/or palmitate was suppressed by silencing NOX4 (Fig. 6, *C* and *D*), strongly suggesting a causal link between NOX4-mediated ROS overproduction and chemotactic factor gene expression. Unexpectedly, pharmacological inhibition of NOX using diphenyleneiodonium (DPI) and apocynin did not inhibit *Saa3* and *Mcp-1* gene expression induced by excess glucose and palmitate, but slightly increased chemotactic factor gene expression (data not shown), suggesting off-target effects.

NADPH Content in Adipocytes Is Induced by High Glucose—NADPH, a co-factor for all the NOX enzymes, is produced in the PPP. To determine the role of the PPP in the generation of ROS and chemotactic factor expression in adipocytes, we first measured NADPH concentrations in 3T3-L1 adipocytes exposed to high glucose and/or palmitate. NADPH concentration was increased after exposure of cells to high glucose but not to palmitate (Fig. 7*A*). Conversely, DHA blocked the increase of NADPH induced by high glucose (Fig. 7*A*). To measure PPP activity, we used [1-^{14}C]glucose and [6-^{14}C]glucose as described previously (31–33). $^{14}CO_2$ production from [1-^{14}C]glucose oxidation was increased by high glucose but not by palmitate (Fig. 7*B*), suggesting oxidation via the PPP in the presence of high glucose. $^{14}CO_2$ production from [6-^{14}C]glucose oxidation only increased after exposure of cells to DHA, suggesting that DHA was oxidized by the Krebs cycle (Fig. 7*B*). Flux through the PPP, which is estimated as $^{14}CO_2$ production from [1-^{14}C]glucose minus $^{14}CO_2$ production from [6-^{14}C]glucose, was only increased by high glucose but not by palmitate or DHA (Fig. 7*B*). Thus, excess glucose could increase the content of NADPH, a co-factor for NOX4 that is generated via the PPP.

Inhibition of PPP Activity Reduces ROS Generation and Chemotactic Factor Gene Expression—To investigate the role of PPP on ROS generation and chemotactic gene expression, we inhibited G6PD, the rate-limiting enzyme of the PPP, using G6PD-specific siRNA and the chemical inhibitors DHEA and 6-AN. We first examined *G6pd* expression levels after exposure

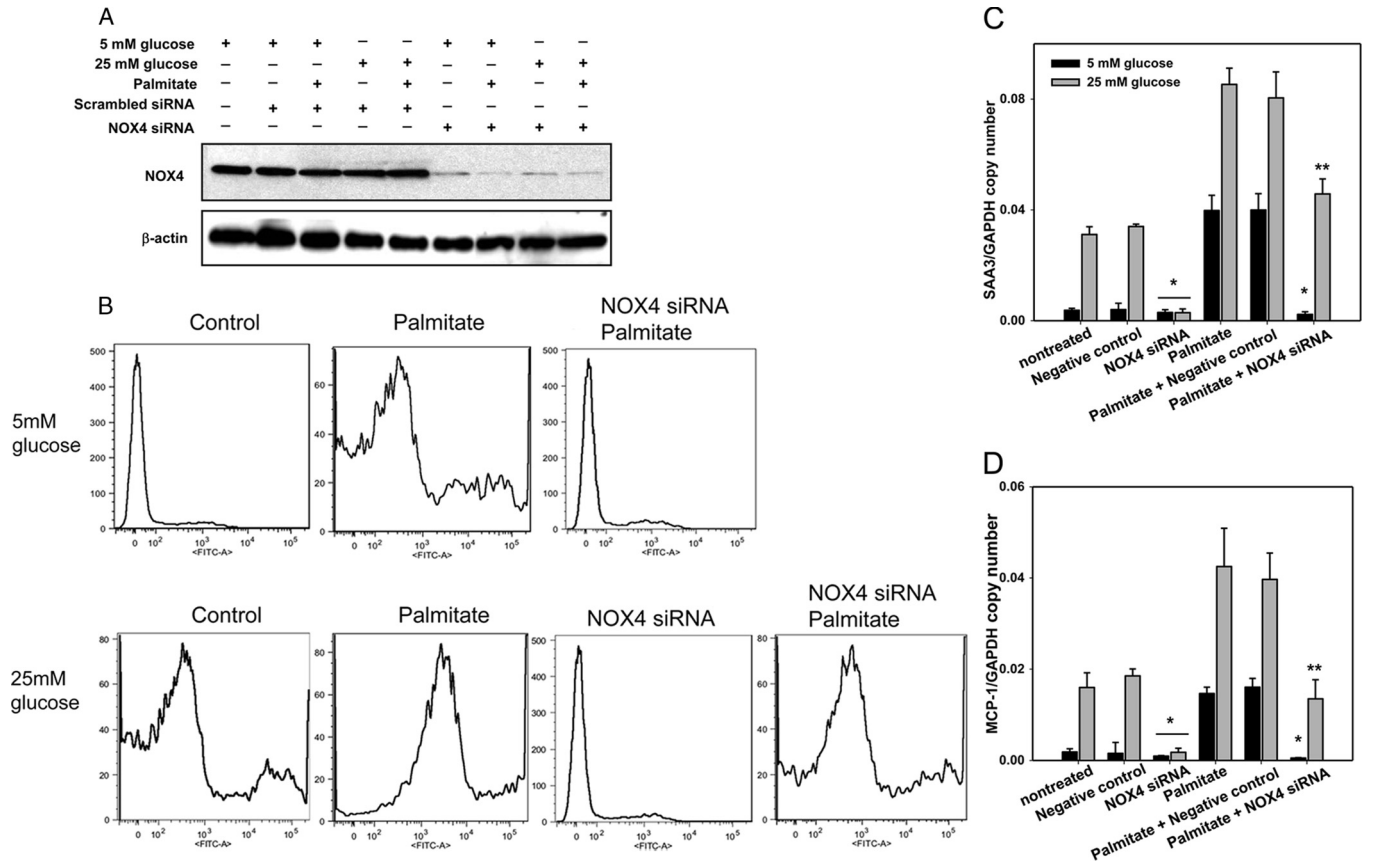

FIGURE 6. **NOX4 silencing inhibits ROS generation and chemotactic factor gene expression induced by excess glucose and palmitate in 3T3-L1 adipocytes.** 3T3-L1 adipocytes were transfected with an siRNA specific for NOX4 or a scrambled siRNA (negative control) as indicated. 24 h later, the cells were exposed to low or high glucose with/without palmitate (250 μM) for 7 days with daily medium changes. *A,* cell lysates were analyzed by immunoblot using a NOX4 antibody and normalized to β-actin. *B,* cells were subjected to FACS analysis using CM-H_2DCFDA. Results are plotted as counts (number of cells) on the *vertical axis versus* DCF fluorescence intensity on the *horizontal axis*. Cells exposed to the indicated treatments are shown in *histograms*. Total RNA was isolated and analyzed by multiplex real time RT-PCR using *Saa3*-specific (*C*) or *Mcp-1*-specific (*D*) primers and normalized to *Gapdh*. *, $p < 0.001$ *versus* negative control in 25 mM glucose, **, $p < 0.001$ *versus* negative control plus palmitate in 25 mM glucose.

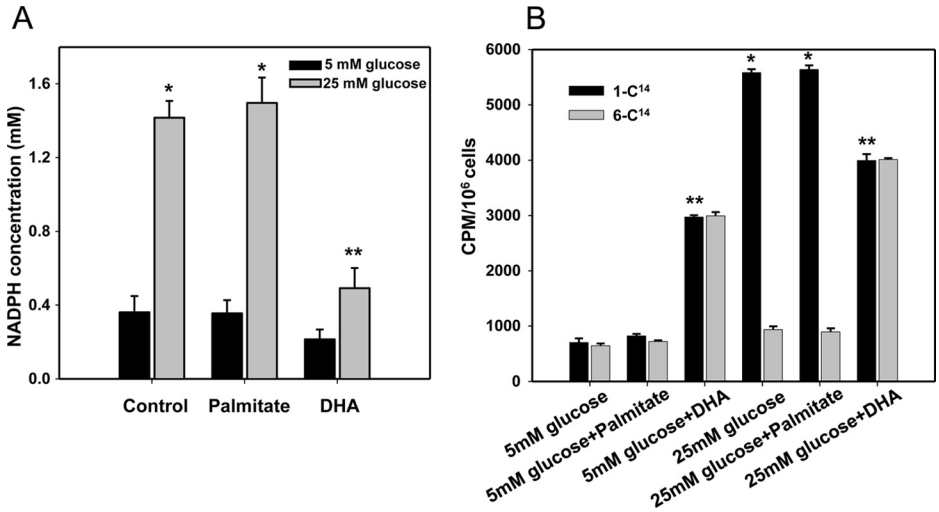

FIGURE 7. **Pentose phosphate pathway activity and NADPH content are increased by excess glucose but not palmitate.** 3T3-L1 adipocytes were exposed to low or high glucose with or without palmitate or DHA (250 μM). At the end of 7 days, some cells were detached and put in vials for glucose oxidation measurement with 0.5 μCi of [1-^{14}C]glucose or [6-^{14}C]glucose. *A,* total cellular NADPH was measured by a NADPH assay kit. *B,* pentose phosphate pathway activity was estimated as $^{14}CO_2$ production from [1-^{14}C]glucose minus $^{14}CO_2$ production [6-^{14}C]glucose after 1 h. *, $p < 0.001$ *versus* 5 mM glucose control. **, $p < 0.001$ *versus* 25 mM glucose control.

of adipocytes to high glucose, palmitate, and DHA, none of which changed *G6pd* expression (data not shown). siRNA transfection decreased G6PD mRNA and protein expression compared with transfection of control siRNA constructs and untreated cells (Fig. 8*A*). G6PD silencing with siRNA or inhibition with DHEA and 6-AN all inhibited the ROS generated by

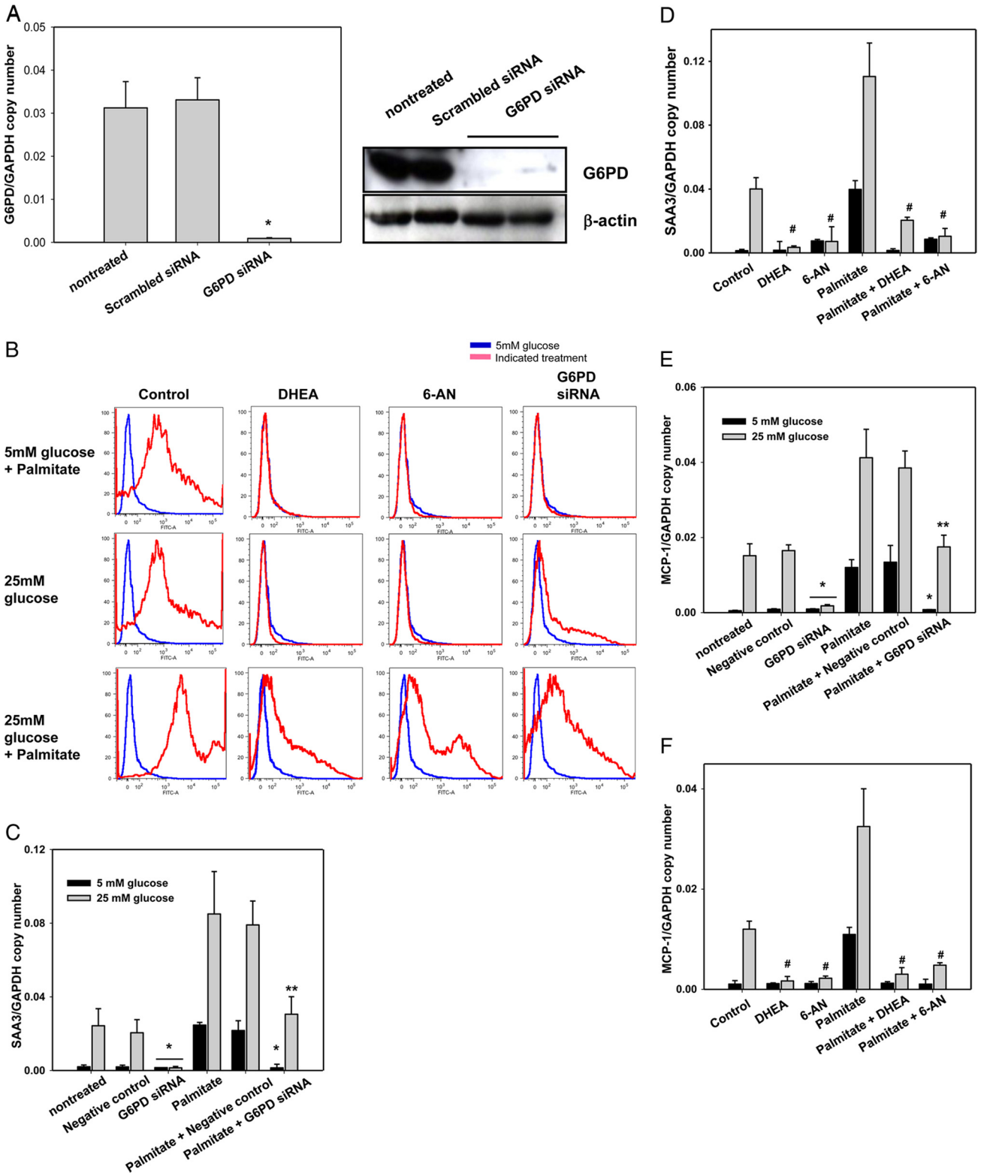

FIGURE 8. **G6PD inhibition blocks the effect of both high glucose and palmitate on ROS generation and chemotactic factor gene expression.** 3T3-L1 adipocytes were exposed to low or high glucose and/or palmitate (250 μM) with or without the G6PD inhibitors, 6-AN (5 μM) or DHEA (100 nM), for 7 days with daily medium changes. For silencing experiments, some 3T3-L1 adipocytes were transfected with an siRNA specific for G6PD or a scrambled siRNA (negative control) as indicated. 24 h later, the cells were exposed to low or high glucose with/without palmitate (250 μM) for 7 days with daily medium changes. *A,* total RNA and lysates from transfected cells were analyzed by multiplex real time RT-PCR using *G6pd*-specific primers and normalized to *Gapdh*, or immunoblot using a G6PD antibody and normalized to β-actin. *B,* FACS analysis was used to sort CM-H_2DCFDA fluorescence in cells. Results are plotted as counts (number of cells) on the *vertical axis versus* DCF fluorescence intensity on the *horizontal axis*. Cells exposed to 5 mM glucose are shown in *blue*, and cells exposed to the indicated treatments are shown in *red*. Total RNA from cells treated with siRNA for G6PD (*C* and *E*), 6-AN and DHEA (*D* and *F*), as described above, was isolated and analyzed by multiplex real time RT-PCR using *Saa3*-specific (*C* and *D*) or *Mcp-1*-specific (*E* and *F*) primers and normalized to *Gapdh*. *, $p < 0.001$ *versus* negative control in 25 mM glucose control; **, $p < 0.001$ *versus* negative control plus palmitate in 25 mM glucose control; #, $p < 0.001$ *versus* 25 mM glucose control.

both high glucose and palmitate (Fig. 8*B*). However, ROS generation induced by exposure to palmitate in the presence of high glucose was only partially inhibited by G6PD silencing (Fig. 8*B*). Moreover, G6PD silencing (Fig. 8, *C* and *E*) and DHEA and 6-AN (Fig. 8, *D* and *F*) all inhibited *Saa3* and *Mcp-1* gene expression induced by both excess glucose as well as palmitate in 3T3-L1 adipocytes, suggesting that NAPDH production by the PPP is involved in NOX4 activity and chemotactic factor gene expression.

Excess Glucose and Palmitate Results in Translocation of NOX4 into Lipid Rafts—Lipid rafts are a part of the plasma membrane and are enriched in cholesterol, sphingolipids, and caveolin. Some proteins are reported to become activated when they move into LRs (36). To determine whether NOX4 is translocated to LRs following exposure of adipocytes to high glucose or palmitate, we isolated LRs by ultracentrifugation. Non-LRs sediment in the lower fractions, while LRs float toward the top of the centrifuge tube. The presence of LRs was judged by detection of caveolin-1 (CAV1). In 5 mM glucose, all NOX4 protein was present in non-LR fractions. However, after exposure to 25 mM glucose, NOX4 proteins translocated into LRs (Fig. 9*A*). Exposure to palmitate also resulted in translocation of NOX4 from non-LRs into LRs (Fig. 9*B*). MβCD, a compound that depletes membrane cholesterol and disrupts LRs, first shifted the CAV1 proteins into the high density non-lipid raft fraction and totally blocked excess glucose- as well as palmitate-induced translocation of NOX4 into LRs (Fig. 9*C*). Moreover, MβCD blocked NOX activity induced by excess glucose and palmitate (Fig. 9*D*) and also inhibited the increase of *Saa3* and *Mcp-1* gene expression induced by palmitate (data not shown). Similarly, DHA also blocked the translocation of NOX4 into LRs induced by excess glucose and palmitate (Fig. 9, *E* and *F*). These results suggest that translocation of NOX4 into LRs may be required for its activation. We also showed that neither DHEA nor 6-AN interfered with the translocation of NOX4 into LRs with or without palmitate stimulation (Fig. 9*G*), suggesting that their effect is due to inhibition of G6PD rather than raft disruption.

To extend our *in vitro* findings in 3T3-L1 adipocytes to *in vivo* models, we isolated cDNA from epididymal adipose tissue from male *ob/ob* and *db/db* mice. *Nox4* mRNA levels were markedly increased in both *ob/ob* and *db/db* mice (Fig. 10) relative to non-obese controls. These findings suggest that NOX4 might also have an important role in adipose tissue inflammation *in vivo*.

DISCUSSION

Our findings indicate that NOX4 is the source of ROS induced by exposure of 3T3-L1 adipocytes to high glucose and palmitate and that mitochondrial oxidation is not involved in ROS generation. Moreover, NOX4-derived ROS leads to increased chemotactic factor gene expression. These findings also indicate that NOX4 activity is regulated by the PPP and translocation into LRs. However, DHA inhibits NOX4 activity by blocking these various mechanisms.

We previously have shown that excess glucose and certain SFAs such as palmitate increase ROS generation, which leads to increased expression of the chemotactic proteins SAA3 and MCP-1 in 3T3-L1 adipocytes, although certain PUFA such as DHA decrease ROS generation and these chemotactic factors (12). Here, we further characterize the source of ROS generated by adipocytes after exposure to increased glucose and SFAs. ROS generation could be enhanced by increased flux through the mitochondrial oxidative phosphorylation pathway in the face of increased utilization of glucose and FFA (37–39). However, FFA that enter adipocytes are rapidly and predominantly converted to fatty acyl-CoA and stored as triglyceride without significant mitochondrial oxidation (40). Increased glucose oxidation in mitochondria could also lead to increased mitochondrial superoxide generation. Prior studies have suggested that quantitatively most carbon atoms derived from glucose do not enter the Krebs cycle, which precedes mitochondrial oxidative phosphorylation (41). Rather, excess energy derived from glucose carbons undergoing glycolysis contributes to lipogenesis, leading to energy storage in fat droplets (41). To test the potential role of mitochondrial oxidation in ROS generation in adipocytes, we evaluated mitochondrial oxidative capacity in several ways. Data from this study confirm that excess glucose does not increase cellular ATP content and mitochondrial oxygen consumption rate, which would argue against increased mitochondrial metabolic flux as a basis for increased adipocyte ROS production. We also showed that intermediary metabolites of the Krebs cycle and acyl-carnitines, which are involved in β-oxidation of fatty acids, did not change after exposure to excess glucose and palmitate, respectively. Moreover, CO_2 released from β-oxidation did not change after exposure of adipocytes to excess glucose and palmitate. In addition, we could not detect any increase in superoxide radicals under high glucose conditions using the MitoSOX probe. Our results also are supported by other studies that show that very little CO_2 ($\sim$2%) was generated via the Krebs cycle in rat adipose tissue and that mitochondrial inhibitors did not reduce ROS generation induced by glucose and palmitate in 3T3-L1 adipocytes (41, 42). Therefore, we conclude that mitochondrial oxidation does not increase ROS generation following exposure of adipocytes to excess glucose and palmitate and that non-mitochondrial sources of ROS generation are likely to have important roles in adipocyte inflammation.

Besides mitochondria, the family of NOX is considered to be an important source of ROS generation (13). NOX are membrane-bound enzyme complexes that transfer electrons from NADPH to oxygen, generating superoxide. This short lived, nonmembrane-permeable ROS is converted to the longer lived membrane-permeable ROS, hydrogen peroxide, predominantly by superoxide dismutase (13). The NOX family has seven isoforms, NOX1, NOX2, NOX3, NOX4, NOX5, DUOX1, and DUOX2 (43). These enzymes can be grouped into $p22^{phox}$-dependent (NOX1–4) and calcium-dependent (NOX5, DUOX1/2) categories. NOX5 and DUOX1/2 require intracellular calcium to activate ROS generation (44, 45). NOX1–4 form stable complexes with membrane-bound $p22^{phox}$, and NOX1–3 require additional cytosolic activators ($p47^{phox}$, $p67^{phox}$, and NOXO1), whereas NOX4 is constitutively active and acts independently of an activator protein (43, 46, 47). It is therefore assumed that NOX1–3 mediates short term effects, while NOX4 is responsible for long term effects. Consistent

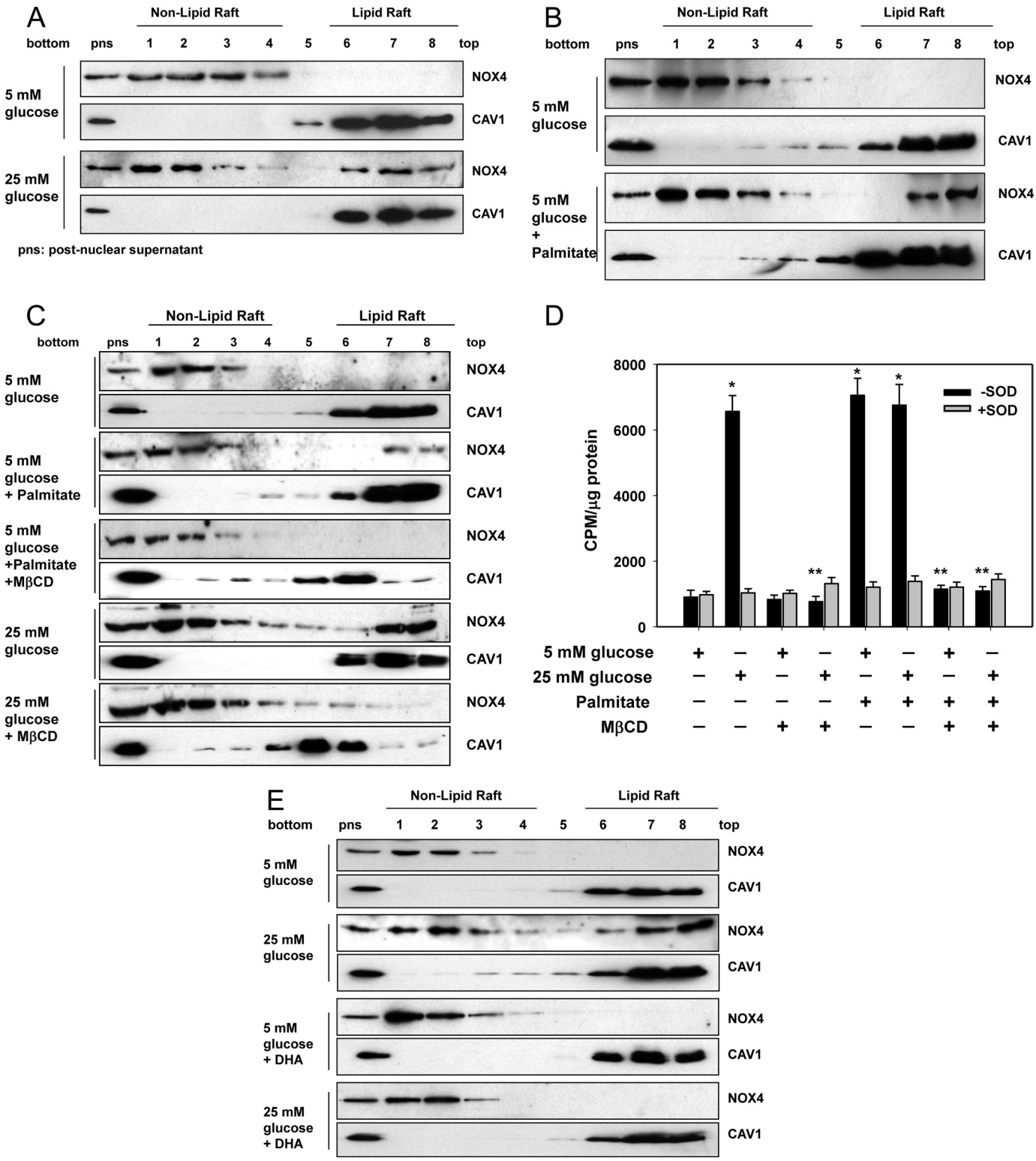

FIGURE 9. **Excess glucose and palmitate induces the translocation of NOX4 to lipid rafts, and MβCD and DHA prevent the translocation of NOX4 in 3T3-L1 adipocytes.** 3T3-L1 adipocytes were exposed to 5 or 25 mM glucose with or without palmitate (250 μM) (*A* and *B*), MβCD (10 μM, *C* and *D*), DHA (250 μM, *E* and *F*), DHEA (100 nM) or 6-AN (5 μM) (*G*) for 7 days with daily medium changes. The LRs were isolated and fractionated by ultracentrifugation using a detergent-free fractionation method. Proteins from OptiPrep-gradient fractions were immunoblotted with anti-NOX4 antibody and anti-caveolin-1 (CAV1) antibody (*A–C* and *E–G*). Fractions 6–8 contain LRs, and fractions 1–4 are non-LR-containing fractions. Membrane fractions obtained by ultracentrifugation were isolated, and NOX activity was measured by NADPH-dependent and SOD-inhibitable lucigenin chemiluminescence assay (*D*). *, $p < 0.001$ *versus* 5 mM glucose control. **, $p < 0.001$ *versus* 25 mM glucose control.

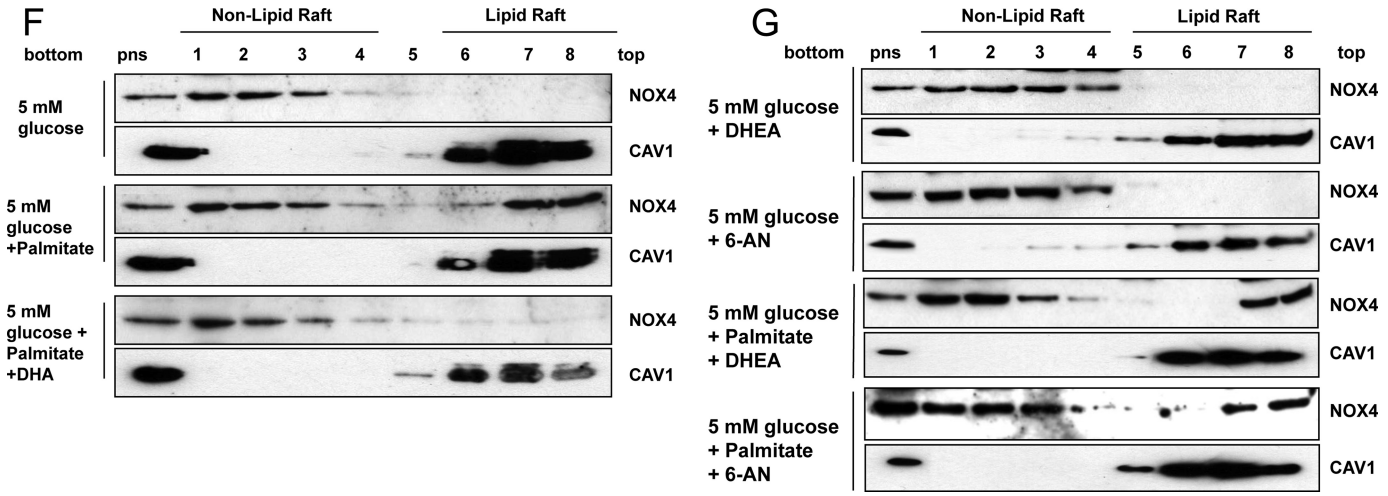

FIGURE 9—*continued*

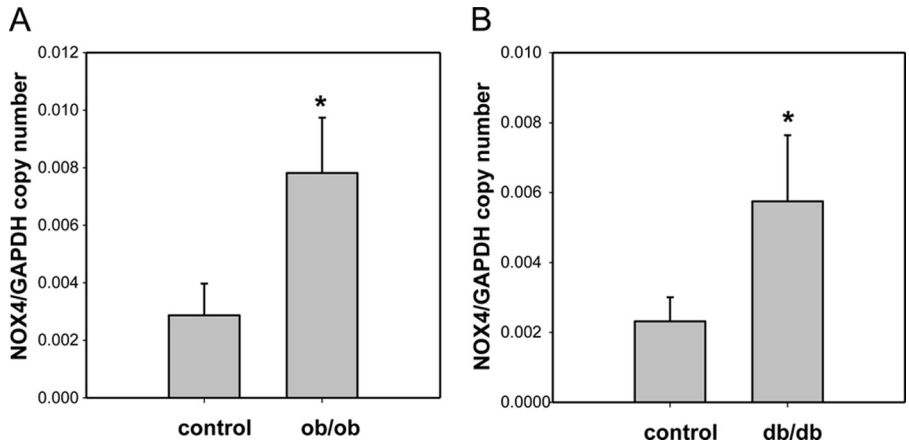

FIGURE 10. **NOX4 mRNA are increased in adipose tissue from genetically obese mice.** *ob/ob* and *db/db* mice and C57BL/6 littermates were fed a chow diet for 24 weeks. Epididymal fat was isolated and analyzed by real time RT-PCR using a *Nox4*-specific primer and probes (*A*, $n = 5$; *B*, $n = 8$). *, $p < 0.001$ *versus* C57BL/6.

with our results, a previous study has shown that NOX inhibitors such as apocynin and DPI, but not mitochondrial inhibitors such as oxypurinol, rotenone, and thenoyltrifluoroacetone, suppressed ROS generation and inflammation in adipocytes exposed to FFA *in vitro* and in adipose tissue from a diet-induced mouse model of obesity (42). However, these studies did not elucidate which NOX isoform accounted for the ROS generation. In our study, we found that *Nox4* is the major *Nox* isoform in differentiated 3T3-L1 adipocytes. Moreover, silencing NOX4 decreased ROS generation stimulated by excess glucose as well as palmitate, leading to inhibition of *Mcp-1* and *Saa3* expression. Thus, NOX4-derived ROS may be a common mediator induced by both excess glucose and palmitate in adipocytes. In our study, NOX4 silencing did not completely block the ROS generation derived from palmitate in the presence of high glucose. Because silencing of NOX4 and G6PD was near complete, as judged by Western blotting and quantitative PCR (Figs. 6*A* and 8*A*), we would expect that the activities of these proteins would be blocked to a considerable extent. However, silencing NOX4 and G6PD or use of chemical inhibitors of G6PD (DHEA and 6-AN) failed to completely block the ROS generated or induction of *Mcp-1* and *Saa3* by palmitate in the presence of high glucose. These findings suggest the existence of other sources of ROS rather than partial knockdown of two important players in common pathway. Unexpectedly, the NOX inhibitors apocynin and DPI failed to suppress ROS generation induced by excess glucose and palmitate. In fact, these inhibitors slightly increased chemotactic factor gene expression. This discrepancy might be due to the fact that DPI and apocynin are nonselective flavoprotein inhibitors, which could also block FAD or NAD oxidases in mitochondria, thereby leading to ROS generation by other disturbances of electron transfer.

To understand how NOX4 is regulated, we first investigated the potential role of the PPP. The PPP generates NADPH and the 5-carbon molecule pentose from the 6-carbon molecule glucose. Because the PPP is major source of cellular NADPH, cells that utilize large amounts of NADPH for fatty acid and steroid biosynthesis (liver, adipose tissue, adrenal cortex, testis, and lactating mammary gland) have high levels of PPP enzymes and produce abundant NADPH. Excess glucose and FFA are stored in the form of triglycerides in fat droplets in adipocytes. Carbon atoms in glucose can be converted to acetyl-CoA via glycolysis and then can undergo lipogenesis prior to storage in fat droplets. Although glucose can be metabolized directly via glycolysis, it can also be metabolized through the PPP, in which

NADPH and pentoses are generated. Adipocytes preferentially metabolize glucose via the PPP, thereby producing abundant NADPH, which is used for lipogenesis (41). Our data showed that NADPH content and activity of the PPP was increased by excess glucose but not palmitate alone in adipocytes. However, inhibition of the PPP by the use of siRNA or chemical inhibitors of the rate-limiting enzyme G6PD suppressed the increase in NOX4 activity that was induced by the combination of glucose and palmitate. Recent studies indicated that G6PD expression is up-regulated in adipose tissue in genetic and diet-induced obesity and that its overexpression is associated with increased adipocyte inflammation and ROS generation (48, 49). Other studies have shown that treatment with DHEA, a G6PD inhibitor, reduces obesity in Zucker diabetic fatty rats (50). Consistent with these observations, our results show that inhibition of G6PD abolishes *Mcp-1* and *Saa3* gene expression and ROS generation induced by excess glucose and palmitate in 3T3-L1 adipocytes, and they support the concept that PPP and G6PD could be modulators or mediators of adipose tissue inflammation. As with the NOX4 silencing experiment, inhibition of G6PDH failed to block completely the ROS induced by palmitate under high glucose conditions, which suggests that other sources of ROS generation are likely to be present when both glucose and palmitate are present concurrently.

LRs are membrane microdomains enriched in glycosylphosphatidylinositol-linked proteins, glycosphingolipids, cholesterol, and caveolin. Caveolae and LRs are involved in protein trafficking and efficient signal transduction (51–53). They serve as compartments for the recruitment of cell signaling components and enzymes to increase the efficient and rapid coupling of receptors. These include some NOX components. In the resting state, NOX2 and $p22^{phox}$ are closely associated with each other in non-LR parts of the cell. Upon activation, they move into LRs and assemble together with the cytosolic activators, $p47^{phox}$ and $p67^{phox}$, thereby forming the active NOX2 enzyme complex that generates superoxide using NADPH (36). Little information was available as to whether NOX4 also moves from the cytoplasm into LRs and, if so, whether this translocation is required for NOX4 to increase ROS generation in adipocytes. Our data show that excess glucose and palmitate increased NOX4 assembly into LRs on the plasma membrane. Disruption of LRs by MβCD blunted ROS formation and diminished chemotactic factor expression. Thus, translocation of NOX4 into LRs appears to play an important role in the generation of ROS mediated by excess glucose and palmitate in adipocytes.

n-3 PUFA in fish oils are postulated to have anti-inflammatory effects (54–56). Previously, we have shown that *n*-3 PUFA, eicosapentaenoate, and DHA inhibited ROS generation, NFκB translocation, and chemotactic factor expression (12). However, the mechanisms of these effects of *n*-3 PUFA were unknown. In this study, we show that DHA can reduce NOX4-derived ROS generation, both by inhibiting PPP activity, thereby leading to decreased availability of NADPH as a co-factor for NOX4, and by disrupting the assembly of NOX4 on plasma membrane LRs.

A limitation of these studies is that they were performed using *in vitro* differentiated 3T3 cells rather than in differentiated stromal vascular cell fraction-derived pre-adipocytes or intact mature adipocytes. However, we also were able to show that NOX4 expression was increased in adipose tissue isolated from mice with two genetic forms of obesity. Adipose tissue contains several cell types in addition to adipocytes, and we were not able to discern which cells are expressing NOX4 *in vivo*, because these studies were performed using whole adipose tissue. Nonetheless, these findings suggest that findings similar to those we observed *in vitro* also occur in intact mice.

In summary, our study implicates ROS generation induced by overnutrition with excess glucose and SFA as playing a pivotal role in the generation of chemotactic factors by adipocytes and on adipocyte inflammation in obesity. NOX4 rather than mitochondrial superoxide overproduction appears to be the source of this ROS generation, which can then trigger a sequence of events that lead to adipose tissue inflammation and insulin resistance. Thus, regulation of NOX4 represents a potential therapeutic target for decreasing adipose tissue inflammation and the accompanying insulin resistance.

REFERENCES

1. Wellen, K. E., and Hotamisligil, G. S. (2003) Obesity-induced inflammatory changes in adipose tissue. *J. Clin. Invest.* **112,** 1785–1788
2. Xu, H., Barnes, G. T., Yang, Q., Tan, G., Yang, D., Chou, C. J., Sole, J., Nichols, A., Ross, J. S., Tartaglia, L. A., and Chen, H. (2003) Chronic inflammation in fat plays a crucial role in the development of obesity-related insulin resistance. *J. Clin. Invest.* **112,** 1821–1830
3. Weisberg, S. P., McCann, D., Desai, M., Rosenbaum, M., Leibel, R. L., and Ferrante, A. W., Jr. (2003) Obesity is associated with macrophage accumulation in adipose tissue. *J. Clin. Invest.* **112,** 1796–1808
4. Bulló, M., García-Lorda, P., Megias, I., and Salas-Salvadó, J. (2003) Systemic inflammation, adipose tissue tumor necrosis factor, and leptin expression. *Obes. Res.* **11,** 525–531
5. Maachi, M., Pieroni, L., Bruckert, E., Jardel, C., Fellahi, S., Hainque, B., Capeau, J., and Bastard, J. P. (2004) Systemic low grade inflammation is related to both circulating and adipose tissue TNFα, leptin, and IL-6 levels in obese women. *Int. J. Obes. Relat. Metab. Disord.* **28,** 993–997
6. Cancello, R., and Clément, K. (2006) Is obesity an inflammatory illness? Role of low grade inflammation and macrophage infiltration in human white adipose tissue. *Bjog* **113,** 1141–1147
7. Houstis, N., Rosen, E. D., and Lander, E. S. (2006) Reactive oxygen species have a causal role in multiple forms of insulin resistance. *Nature* **440,** 944–948
8. Evans, J. L., Goldfine, I. D., Maddux, B. A., and Grodsky, G. M. (2002) Oxidative stress and stress-activated signaling pathways: a unifying hypothesis of type 2 diabetes. *Endocr. Rev.* **23,** 599–622
9. Hansen, L. L., Ikeda, Y., Olsen, G. S., Busch, A. K., and Mosthaf, L. (1999) Insulin signaling is inhibited by micromolar concentrations of H_2O_2. Evidence for a role of H_2O_2 in tumor necrosis factor α-mediated insulin resistance. *J. Biol. Chem.* **274,** 25078–25084
10. Inoguchi, T., Li, P., Umeda, F., Yu, H. Y., Kakimoto, M., Imamura, M., Aoki, T., Etoh, T., Hashimoto, T., Naruse, M., Sano, H., Utsumi, H., and Nawata, H. (2000) High glucose level and free fatty acid stimulate reactive oxygen species production through protein kinase C-dependent activation of NAD(P)H oxidase in cultured vascular cells. *Diabetes* **49,** 1939–1945
11. Foncea, R., Carvajal, C., Almarza, C., and Leighton, F. (2000) Endothelial cell oxidative stress and signal transduction. *Biol. Res.* **33,** 89–96
12. Yeop Han, C., Kargi, A. Y., Omer, M., Chan, C. K., Wabitsch, M., O'Brien, K. D., Wight, T. N., and Chait, A. (2010) Differential effect of saturated and unsaturated free fatty acids on the generation of monocyte adhesion and chemotactic factors by adipocytes. Dissociation of adipocyte hypertrophy from inflammation. *Diabetes* **59,** 386–396

13. Bedard, K., and Krause, K. H. (2007) The NOX family of ROS-generating NADPH oxidases. Physiology and pathophysiology. *Physiol. Rev.* **87,** 245–313
14. Hecker, L., Vittal, R., Jones, T., Jagirdar, R., Luckhardt, T. R., Horowitz, J. C., Pennathur, S., Martinez, F. J., and Thannickal, V. J. (2009) NADPH oxidase-4 mediates myofibroblast activation and fibrogenic responses to lung injury. *Nat. Med.* **15,** 1077–1081
15. Bolterman, R. J., Manriquez, M. C., Ortiz Ruiz, M. C., Juncos, L. A., and Romero, J. C. (2005) Effects of captopril on the renin angiotensin system, oxidative stress, and endothelin in normal and hypertensive rats. *Hypertension* **46,** 943–947
16. Dikalov, S. I., Dikalova, A. E., Bikineyeva, A. T., Schmidt, H. H., Harrison, D. G., and Griendling, K. K. (2008) Distinct roles of Nox1 and Nox4 in basal and angiotensin II-stimulated superoxide and hydrogen peroxide production. *Free Radic. Biol. Med.* **45,** 1340–1351
17. Vallet, P., Charnay, Y., Steger, K., Ogier-Denis, E., Kovari, E., Herrmann, F., Michel, J. P., and Szanto, I. (2005) Neuronal expression of the NADPH oxidase NOX4, and its regulation in mouse experimental brain ischemia. *Neuroscience* **132,** 233–238
18. Lin, Y., Berg, A. H., Iyengar, P., Lam, T. K., Giacca, A., Combs, T. P., Rajala, M. W., Du, X., Rollman, B., Li, W., Hawkins, M., Barzilai, N., Rhodes, C. J., Fantus, I. G., Brownlee, M., and Scherer, P. E. (2005) The hyperglycemia-induced inflammatory response in adipocytes. The role of reactive oxygen species. *J. Biol. Chem.* **280,** 4617–4626
19. Han, C. Y., Chiba, T., Campbell, J. S., Fausto, N., Chaisson, M., Orasanu, G., Plutzky, J., and Chait, A. (2006) Reciprocal and coordinate regulation of serum amyloid A *versus* apolipoprotein A-I and paraoxonase-1 by inflammation in murine hepatocytes. *Arterioscler. Thromb. Vasc. Biol.* **26,** 1806–1813
20. Goueffic, Y., Potter-Perigo, S., Chan, C. K., Johnson, P. Y., Braun, K., Evanko, S. P., and Wight, T. N. (2007) Sirolimus blocks the accumulation of hyaluronan (HA) by arterial smooth muscle cells and reduces monocyte adhesion to the ECM. *Atherosclerosis* **195,** 23–30
21. Han, C. Y., Subramanian, S., Chan, C. K., Omer, M., Chiba, T., Wight, T. N., and Chait, A. (2007) Adipocyte-derived serum amyloid A3 and hyaluronan play a role in monocyte recruitment and adhesion. *Diabetes* **56,** 2260–2273
22. Chang, M. Y., Han, C. Y., Wight, T. N., and Chait, A. (2006) Antioxidants inhibit the ability of lysophosphatidylcholine to regulate proteoglycan synthesis. *Arterioscler. Thromb. Vasc. Biol.* **26,** 494–500
23. Quijano, C., Castro, L., Peluffo, G., Valez, V., and Radi, R. (2007) Enhanced mitochondrial superoxide in hyperglycemic endothelial cells. Direct measurements and formation of hydrogen peroxide and peroxynitrite. *Am. J. Physiol. Heart Circ. Physiol.* **293,** H3404–H3414
24. Golej, D. L., Askari, B., Kramer, F., Barnhart, S., Vivekanandan-Giri, A., Pennathur, S., and Bornfeldt, K. E. (2011) Long chain acyl-CoA synthetase 4 modulates prostaglandin E_2 release from human arterial smooth muscle cells. *J. Lipid Res.* **52,** 782–793
25. Lemons, J. M., Feng, X. J., Bennett, B. D., Legesse-Miller, A., Johnson, E. L., Raitman, I., Pollina, E. A., Rabitz, H. A., Rabinowitz, J. D., and Coller, H. A. (2010) Quiescent fibroblasts exhibit high metabolic activity. *PLoS Biol.* **8,** e1000514
26. Koves, T. R., Ussher, J. R., Noland, R. C., Slentz, D., Mosedale, M., Ilkayeva, O., Bain, J., Stevens, R., Dyck, J. R., Newgard, C. B., Lopaschuk, G. D., and Muoio, D. M. (2008) Mitochondrial overload and incomplete fatty acid oxidation contribute to skeletal muscle insulin resistance. *Cell Metab.* **7,** 45–56
27. Sweet, I. R., Cook, D. L., Wiseman, R. W., Greenbaum, C. J., Lernmark, A., Matsumoto, S., Teague, J. C., and Krohn, K. A. (2002) Dynamic perifusion to maintain and assess isolated pancreatic islets. *Diabetes Technol. Ther.* **4,** 67–76
28. Sweet, I. R., Khalil, G., Wallen, A. R., Steedman, M., Schenkman, K. A., Reems, J. A., Kahn, S. E., and Callis, J. B. (2002) Continuous measurement of oxygen consumption by pancreatic islets. *Diabetes Technol. Ther.* **4,** 661–672
29. Kohanski, R. A., Frost, S. C., and Lane, M. D. (1986) Insulin-dependent phosphorylation of the insulin receptor-protein kinase and activation of glucose transport in 3T3-L1 adipocytes. *J. Biol. Chem.* **261,** 12272–12281
30. Smart, E. J., Ying, Y. S., Mineo, C., and Anderson, R. G. (1995) A detergent-free method for purifying caveolae membrane from tissue culture cells. *Proc. Natl. Acad. Sci. U.S.A.* **92,** 10104–10108
31. Katz, J., and Wood, H. G. (1960) The use of glucose-C14 for the evaluation of the pathways of glucose metabolism. *J. Biol. Chem.* **235,** 2165–2177
32. Rodbell, M. (1964) Metabolism of isolated fat cells. I. Effects of hormones on glucose metabolism and lipolysis. *J. Biol. Chem.* **239,** 375–380
33. Olefsky, J. M. (1977) Mechanisms of decreased insulin responsiveness of large adipocytes. *Endocrinology* **100,** 1169–1177
34. Marette, A., and Bukowiecki, L. J. (1991) Noradrenaline stimulates glucose transport in rat brown adipocytes by activating thermogenesis. Evidence that fatty acid activation of mitochondrial respiration enhances glucose transport. *Biochem. J.* **277,** 119–124
35. Cominacini, L., Pasini, A. F., Garbin, U., Davoli, A., Tosetti, M. L., Campagnola, M., Rigoni, A., Pastorino, A. M., Lo Cascio, V., and Sawamura, T. (2000) Oxidized low density lipoprotein (ox-LDL) binding to ox-LDL receptor-1 in endothelial cells induces the activation of NF-κB through an increased production of intracellular reactive oxygen species. *J. Biol. Chem.* **275,** 12633–12638
36. Li, H., Han, W., Villar, V. A., Keever, L. B., Lu, Q., Hopfer, U., Quinn, M. T., Felder, R. A., Jose, P. A., and Yu, P. (2009) D1-like receptors regulate NADPH oxidase activity and subunit expression in lipid raft microdomains of renal proximal tubule cells. *Hypertension* **53,** 1054–1061
37. Nishikawa, T., Edelstein, D., Du, X. L., Yamagishi, S., Matsumura, T., Kaneda, Y., Yorek, M. A., Beebe, D., Oates, P. J., Hammes, H. P., Giardino, I., and Brownlee, M. (2000) Normalizing mitochondrial superoxide production blocks three pathways of hyperglycemic damage. *Nature* **404,** 787–790
38. Tsung, A., Klune, J. R., Zhang, X., Jeyabalan, G., Cao, Z., Peng, X., Stolz, D. B., Geller, D. A., Rosengart, M. R., and Billiar, T. R. (2007) HMGB1 release induced by liver ischemia involves Toll-like receptor 4 dependent reactive oxygen species production and calcium-mediated signaling. *J. Exp. Med.* **204,** 2913–2923
39. Patel, C., Ghanim, H., Ravishankar, S., Sia, C. L., Viswanathan, P., Mohanty, P., and Dandona, P. (2007) Prolonged reactive oxygen species generation and nuclear factor-κB activation after a high fat, high carbohydrate meal in the obese. *J. Clin. Endocrinol. Metab.* **92,** 4476–4479
40. Frayn, K. N., Langin, D., and Karpe, F. (2008) Fatty acid-induced mitochondrial uncoupling in adipocytes is not a promising target for treatment of insulin resistance unless adipocyte oxidative capacity is increased. *Diabetologia* **51,** 394–397
41. Katz, J., Landau, B. R., and Bartsch, G. E. (1966) The pentose cycle, triose phosphate isomerization, and lipogenesis in rat adipose tissue. *J. Biol. Chem.* **241,** 727–740
42. Furukawa, S., Fujita, T., Shimabukuro, M., Iwaki, M., Yamada, Y., Nakajima, Y., Nakayama, O., Makishima, M., Matsuda, M., and Shimomura, I. (2004) Increased oxidative stress in obesity and its impact on metabolic syndrome. *J. Clin. Invest.* **114,** 1752–1761
43. Kawahara, T., Quinn, M. T., and Lambeth, J. D. (2007) Molecular evolution of the reactive oxygen-generating NADPH oxidase (Nox/Duox) family of enzymes. *BMC Evol. Biol.* **7,** 109
44. Bánfi, B., Molnár, G., Maturana, A., Steger, K., Hegedûs, B., Demaurex, N., and Krause, K. H. (2001) A Ca^{2+}-activated NADPH oxidase in testis, spleen, and lymph nodes. *J. Biol. Chem.* **276,** 37594–37601
45. Dupuy, C., Ohayon, R., Valent, A., Noël-Hudson, M. S., Dème, D., and Virion, A. (1999) Purification of a novel flavoprotein involved in the thyroid NADPH oxidase. Cloning of the porcine and human cDNAs. *J. Biol. Chem.* **274,** 37265–37269
46. Martyn, K. D., Frederick, L. M., von Loehneysen, K., Dinauer, M. C., and Knaus, U. G. (2006) Functional analysis of Nox4 reveals unique characteristics compared with other NADPH oxidases. *Cell. Signal.* **18,** 69–82
47. Ambasta, R. K., Kumar, P., Griendling, K. K., Schmidt, H. H., Busse, R., and Brandes, R. P. (2004) Direct interaction of the novel Nox proteins with p22phox is required for the formation of a functionally active NADPH oxidase. *J. Biol. Chem.* **279,** 45935–45941
48. Park, J., Rho, H. K., Kim, K. H., Choe, S. S., Lee, Y. S., and Kim, J. B. (2005) Overexpression of glucose-6-phosphate dehydrogenase is associated with lipid dysregulation and insulin resistance in obesity. *Mol. Cell. Biol.* **25,** 5146–5157

49. Park, J., Choe, S. S., Choi, A. H., Kim, K. H., Yoon, M. J., Suganami, T., Ogawa, Y., and Kim, J. B. (2006) Increase in glucose-6-phosphate dehydrogenase in adipocytes stimulates oxidative stress and inflammatory signals. *Diabetes* **55,** 2939–2949
50. Cleary, M. P., and Zisk, J. F. (1986) Anti-obesity effect of two different levels of dehydroepiandrosterone in lean and obese middle-aged female Zucker rats. *Int. J. Obes.* **10,** 193–204
51. Simons, K., and Ikonen, E. (1997) Functional rafts in cell membranes. *Nature* **387,** 569–572
52. Smart, E. J., and Anderson, R. G. (2002) Alterations in membrane cholesterol that affect structure and function of caveolae. *Methods Enzymol.* **353,** 131–139
53. Allen, J. A., Halverson-Tamboli, R. A., and Rasenick, M. M. (2007) Lipid raft microdomains and neurotransmitter signaling. *Nat. Rev. Neurosci.* **8,** 128–140
54. Krey, G., Braissant, O., L'Horset, F., Kalkhoven, E., Perroud, M., Parker, M. G., and Wahli, W. (1997) Fatty acids, eicosanoids, and hypolipidemic agents identified as ligands of peroxisome proliferator-activated receptors by coactivator-dependent receptor ligand assay. *Mol. Endocrinol.* **11,** 779–791
55. Li, H., Ruan, X. Z., Powis, S. H., Fernando, R., Mon, W. Y., Wheeler, D. C., Moorhead, J. F., and Varghese, Z. (2005) EPA and DHA reduce LPS-induced inflammation responses in HK-2 cells. Evidence for a PPAR-γ-dependent mechanism. *Kidney Int.* **67,** 867–874
56. Neschen, S., Morino, K., Rossbacher, J. C., Pongratz, R. L., Cline, G. W., Sono, S., Gillum, M., and Shulman, G. I. (2006) Fish oil regulates adiponectin secretion by a peroxisome proliferator-activated receptor-γ-dependent mechanism in mice. *Diabetes* **55,** 924–928